Tetrahedron Vol. 40, No. 3, pp 579 to 592, 1984
Printed in Great Britain.

0040-4020/84 $3.00 + 00
Pergamon Press Ltd.

CYCLOPHANE PORPHYRINS AND THEIR METAL COMPLEXES[1]

BIOMIMETIC STUDY ON RECEPTOR SITE OF HEMOPROTEIN OXYGEN BINDING

HISANOBU OGOSHI,*[2a] HIROSHI SUGIMOTO,[2b] MASAO MIYAKE[2c] and ZEN-ICHI YOSHIDA*[2c]
Department of Synthetic Chemistry, Faculty of Engineering, Kyoto University, Yoshida, Kyoto 606, Japan

(*Received in U.S.A. October* 1982)

Abstract—A new symmetric porphyrin, 7,8,17,18-tetraethyl-3,13-dimethylporphyrin-2,12-dipropionic acid and its derivatives were synthesized by the a,c-biladiene route. Condensation of the dipropionic acid with diamine, $[H_2N(CH_2)_nNH_2$, n = 6,7,8,9,10,12, and 14], afforded the corresponding cyclophane porphyrins. The bridged groups were characterized by the ^{1}H-NMR spectra of their zinc complexes. The spin state of the Fe(III) complexes of the cyclophane porphyrins was investigated by changing the size of the bridged chain or size of axial ligand. The cyclophane-porphyrinato(III) perchlorate complexes in a mixture of MeOH and $CHCl_3$ with 4-benzylpyridine provide a model for methemoproteins. Steric constraint between an axial ligand and the bridge group, $[-CH_2CH_2CONH(CH_2)_nNHCOCH_2CH_2]$ at the bridged face determines the ratio of the penta- and hexa-coordinated ferric complexes. The rate of O-binding to the Co(II) cyclophane porphyrins is markedly dependent on the size of the bridge chain. The present result indicates that removal of a solvent molecule or sixth axial ligand from the near proximity of the Co(II) complex increases the rate of O- binding.

Syntheses of various kinds of porphyrins and metalloporphyrins have been developed in order to elucidate the functions of the heme enzymes and hemoproteins. In monomeric porphyrin ligands, special synthetic devices have been developed to construct a hydrophobic environment in close proximity to the metal atom in the metalloporphyrins. The main purpose of such a systhetic design is to avoid autooxidation of the oxyheme.[3-7] Approaches to synthetic porphyrin ligands as models for hemoproteins can be classified into two groups. The first approach involves the synthesis of *meso*-tetra-(2-substituted-phenyl)porphyrins; examples are the picket fence,[3] capped,[4] and *strati* porphyrins.[5] While the second involves the synthesis of porphyrins having strapped axial ligands or bridged chains at the peripheral β-positions of the pyrrole ring of the porphyrin.[6] These porphyrins have proven to be very useful models to mimic the heme enzymes and hemoproteins. In previous communications, we have demonstrated the marked effect of the bridged group on axial ligation in cyclophane porphyrin iron complexes.[7] Battersby *et al.* have reported independent syntheses of bridged porphyrins.[8] More recently Chang *et al.* have also made similar bridged porphyrins ("crowned porphyrins"[9,10]) and investigated nonbonding steric effect on CO and O_2 binding to the heme.[10]. Brief reports of the syntheses and physicochemical properties of doubly bridged porphyrins has also approved.[11,12]

Furthermore, from the standpoint of cyclophane chemistry, it is very interesting to note the physicochemical properties of large aromatic compounds bridged with long chains. We wish to report the syntheses of several cyclophane porphyrins and their metalloporphyrins. In particular, anomalous axial ligation to the cyclophane porphyrin complexes will be described in relation to some stage of the hemoproteins and heme enzymes which usual metalloporphyrins are not able to mimic.

RESULTS AND DISCUSSION

Two 3,4-diethylpyrroles constitute the A and C rings in the cyclophane porphyrin as is shown in the Scheme 1. Battersby *et al.* have used 2-methyl-3-ethylpyrrole instead of 3,4-di-ethylpyrrole to construct bridged porphyrins.[12] However, there is no essential difference between the two systems as ligands. Dipyrrylmethene (**3**) was prepared by the condensation of **1** and **2** in 48% HBr-EtOH. Bromination of **3** at the 5-position of the pyrrole ring and at the 5'-Me was carried out with Br_2 in glacial acetic acid. The a,c-biladiene (**5**) was obtained in good yield by coupling of dipyrrylmethene (**3** and **4**) with anhydrous stannic chloride. The diester (**6**) was prepared in moderate yield from the cyclization of **5** in *o*-dichlorobenzene at elevated temperature. Hydrolysis of the diester (**6**) in acidic media gave the carboxylate (**7**). Reduction of **6** with $LiAlH_4$ afforded diol (**8**), which was converted to the dibromide (**9**) in aqueous HBr. The porphyrin (**7**) was strapped by condensation of two propionic acid groups at the 2- and 12-positions with diamine $H_2N(CH_2)_nNH_2$ in high dilution. Therefore, the bridged chain $[-CH_2CH_2CONH(CH_2)_nNHCOCH_2CH_2-]$ has n + 8 atoms. (The number in the bracket of [*m*]-cyclophane porphyrin denotes the total number of atoms in the bridge chain across the face of the porphyrin ring.) Yields of the cyclophane porphyrins were improved by the mixed anhydride method. The cyclophane porphyrins were separated in the form of their Zn(II) complexes due to facile manipulation in TLC. A reference porphyrin was prepared by condensation of **6** with n-hexylamine in order to compare the physical properties of the cyclophane porphyrins with those of unbridged porphyrins. Mass spectra of the Zn(II)

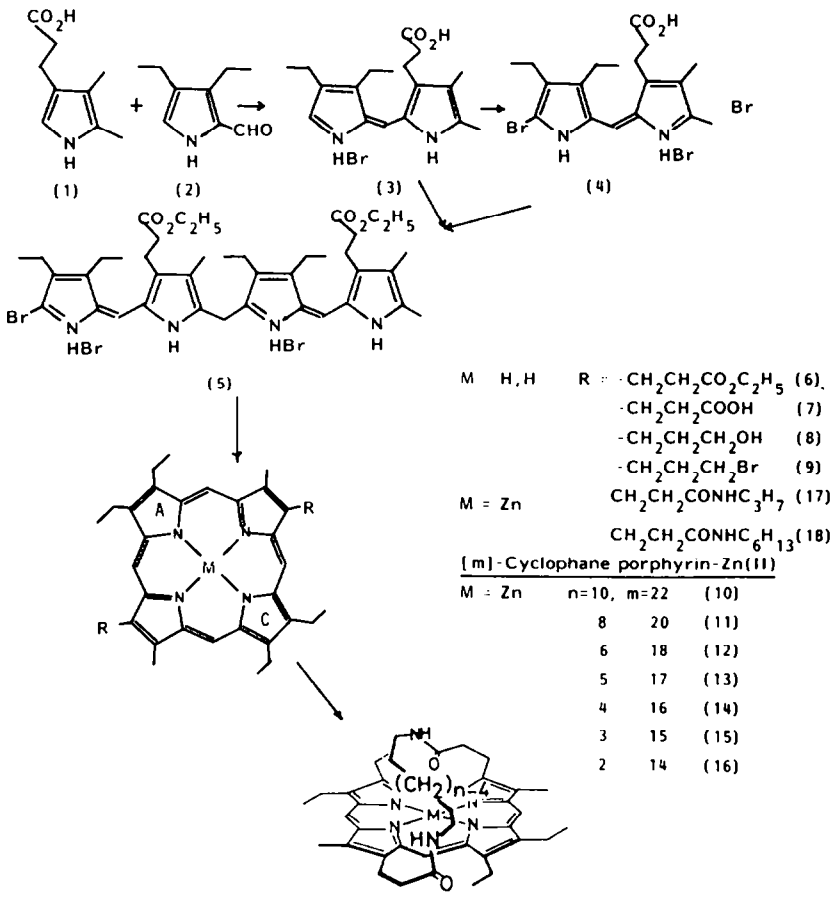

Scheme 1.

complexes show parent peaks at the expected mass and weak peaks due to the doubly charged ions. The absorption spectra of the cyclophane porphyrins are almost identical with that of the reference porphyrin.

Fig. 1 shows the ^{1}H-NMR spectra of the Zn(II) complex of [22]-cyclophane porphyrin (**10**) at 32 and 90° in pyridine-d_5. Fig. 2 displays those of the Zn(II) complex of [14]-cyclophane porphyrin (**16**) under the same conditions. Some chemical shifts of the complex (**10**) appear at higher magnetic field by about 1 ppm than those of the reference complex. These signals are assignable to the CH_2 groups of the bridged chain. The distance between the central methylene groups and the Zn atom is estimated to be 7 Å from the small observed up-field shift on the basis of the isoschielding map of the alkyl Rh(III) porphyrin complex.[14] In contrast to [22]-cyclophane porphyrin, the NMR spectra of the porphyrin complexes strapped by shorter chains show marked high-field shifts due to the diamagnetic ring current of the porphyrin macrocycle. The chemical shifts of the hexamethylene protons of **16** are observed at δ -1.6, -2.2 and -2.7. Those of the methylene groups of **15** are centered at δ -1.0, -2.6 and -3.6. The chemical shifts of the central methylene of the heptamethylene chain showed the largest up-field shift among those of the cyclophane porphyrin complexes. The separation of the central methylene group of **15** from the Zn atom is estimated to be 4 Å from the isoshielding map.[14]

It is noted that some signals become sharper at elevated temperature. Broad signals due to the methylene groups of the[18]-cyclophane complex at 32° are resolved into fine structures at 90° in pyridine-d_5 solution. The signals of the α- and β-CH_2 protons at 5.0 and 3.4 and the δ-CH_2 at 2.9 became clearer and sharper at elevated temperature as is seen in Fig. 3. These trends are indicative of averaging of the methylene sites due to fast thermal motion of the bridged chain. The signals of the amide NH protons shift toward higher magnetic field by 1–2 ppm as the temperature is increased. This up-field shift of the amide proton resonance is probably caused by a wiggling motion of the bridged chain at higher temperature. The average location of the NH proton of the rather rigid amide group seems to be in close proximity to the porphyrin plane in the thermally activated state. Fig. 4 illustrates a schematic representation of the proton chemical shifts of the bridged chains. The reference porphyrin complex (**17**) shows two triplets at 5.30 and 6.61 ppm assigned to the $-^{\alpha}CH_2-$ and $-^{\beta}CH_2-$ protons of the propionamide groups. Those of the cyclophane complexes become more complicated and may be analyzed as an AA′BB′ type pattern. These results clearly indicate that the free rotation of the propionamide around the pyrrolic C and the α-C of the bridge is entirely inhibited. All signals of the bridged methylene groups represented by the δ- and ϵ-protons are shifted to lower magnetic field as the number of methylenes increases. The shielding effect due to the diamagnetic ring current may, therefore, be used to estimate the cavity size at the bridged face of the porphyrin complexes.

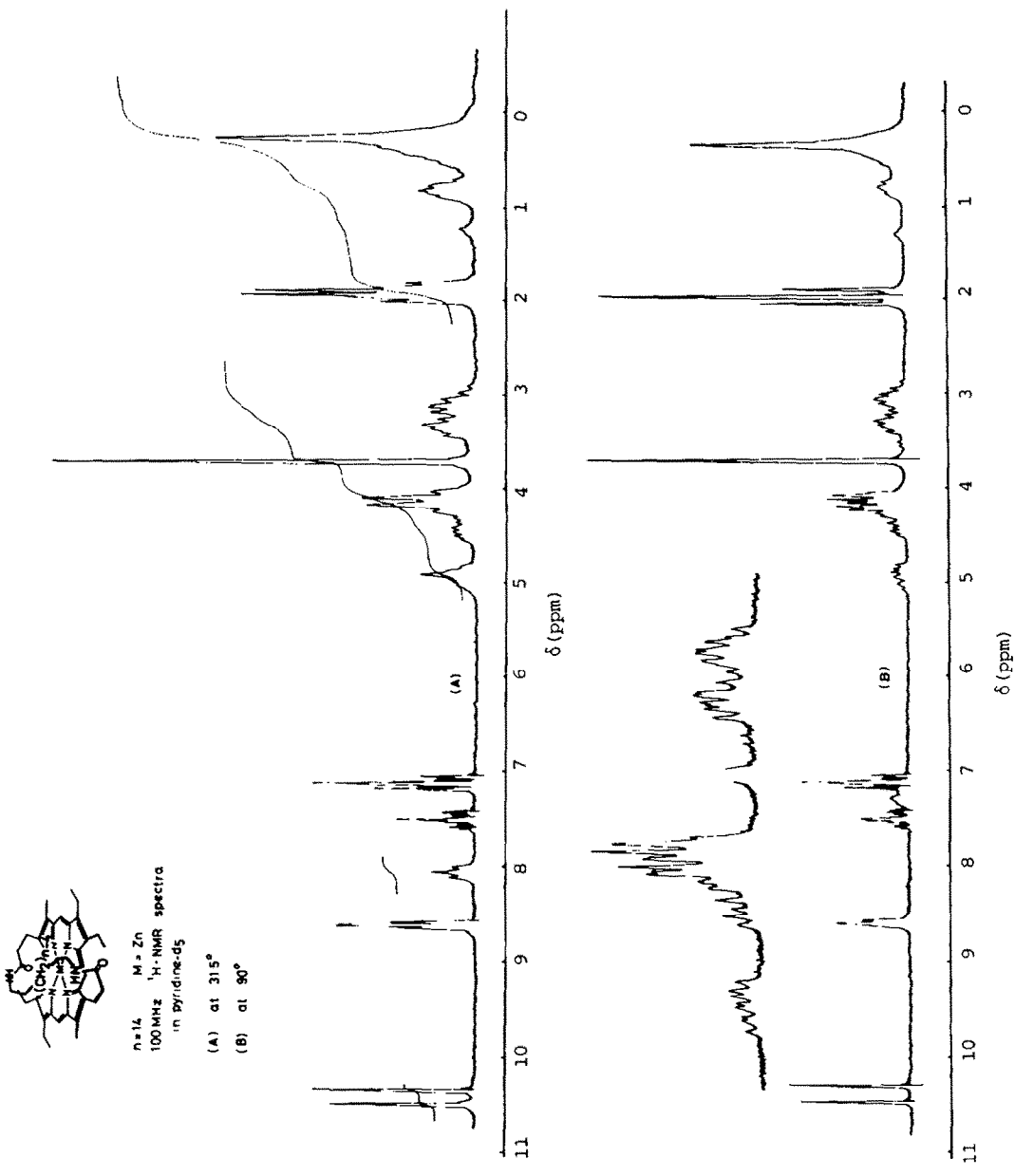

Fig. 1. ^{1}H NMR spectra of [22]-cyclophane porphyrin Zn(II) complex in pyridine-d_5 at 31.5° and 90°.

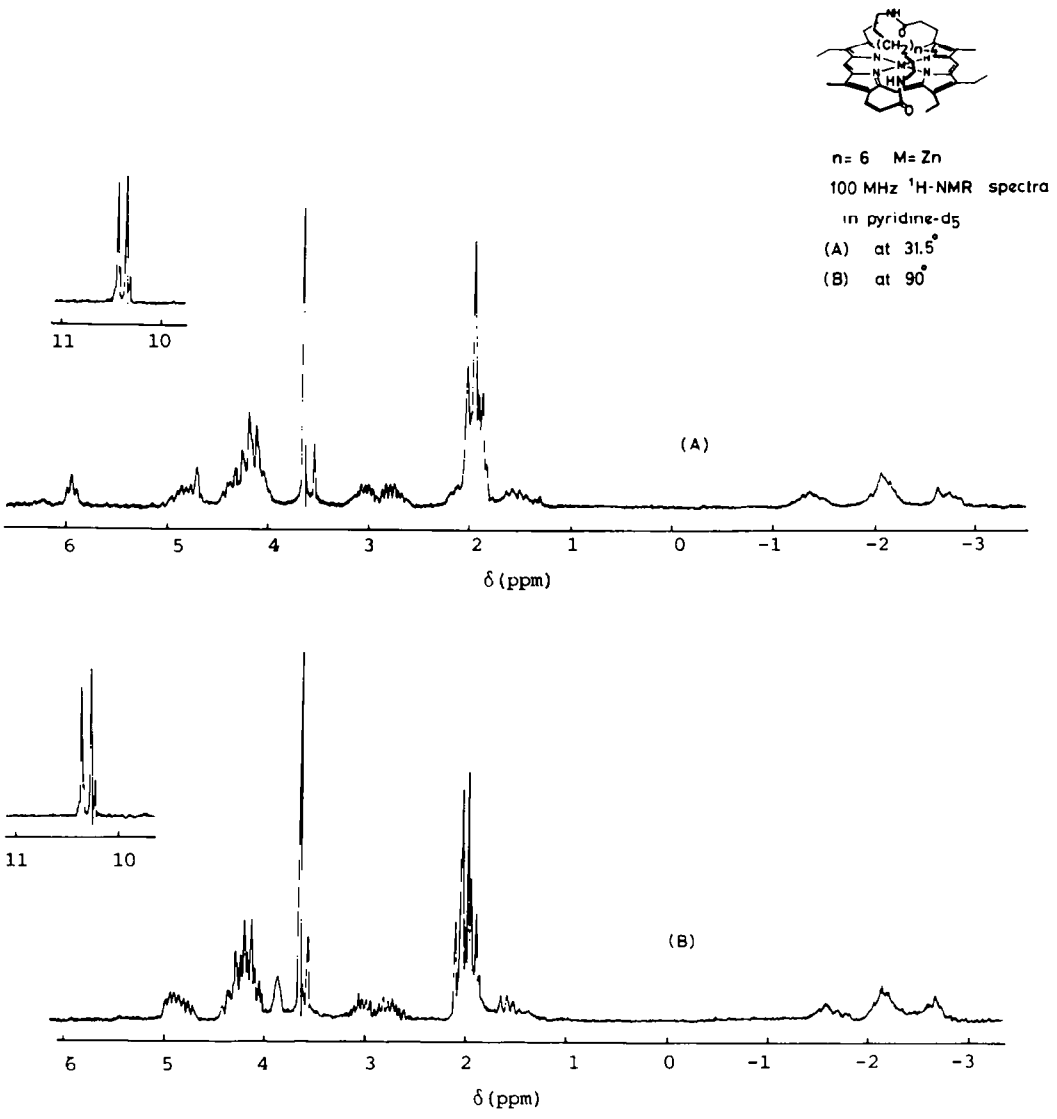

Fig. 2. ^{1}H NMR spectra of [14]-cyclophane porphyrin Zn(II) complex in pyridine-d_5 at 31.5° and 90°.

Iron complexes of cyclophane porphyrins

It is well known that ferric porphyrins exist in the high spin (s = 5/2) or in the low spin state (s = 1/2) in the presence of amines such as pyridine and imidazole. Penta-coordinated ferric porphyrin such as chlorohemin are typically high spin. Axial ligation of two amines to ferric complexes generates the hexa-coordinated low spin ferric porphyrins. It is anticipated that steric constraint between the axial ligand and the bridged chain group may restrict axial ligation of the 6th ligand at the bridged face. This in turn implies that equilibrium between high and low spin states is dependent upon both the size of the axial ligand and the length of the bridged chain. In our previous communication we have noted the effect of the size of axial ligand on spin equilibrium in the ferric porphyrins[7b] and the effect of the bridged chain length on the spin equilibrium of ferrous porphyrins for low (s = 0) and high (s = 2) spin states.[7c] Figure 5 shows sharp contrasts in the visible spectra of the ferric complexes of [14]-cyclophaneporphyrin (**25**) and the reference porphyrin (**29**). The absorption spectrum of the ferric complex of (**25**) in $CHCl_3$ is characteristic of the high spin state. Even in pyridine solution, the spectrum of **25** is identical with that in the $CHCl_3$ solution. While the ferric high spin complex of the reference porphyrin (**18**) is readily converted to the hexa-coordinated complex in pyridine solution. Steric hindrance at the bridged face apparently inhibits coordination of pyridine. Figure 6 indicates absorption spectra of [14]- and [22]-cyclophane porphyrin Fe(II) complexes in pyridine and those of [22]-cyclophaneporphyrin Fe(II) complex in 4-t-butylpyridine. The spectral features of the ferrous complex obtained from **25** in pyridine is characteristic of the low spin complex, hemochrome (Scheme 2, E). As is expected, ligation of rather bulky axial ligands such as 4-t-butylpyridine results in formation of the deoxy form (Scheme 2, **B**). The dioxygen Fe(II) complex of the cyclophane porphyrins (Scheme 2, C) were unstable, forming μ-oxocomplex at the open face (Scheme 2, G) at

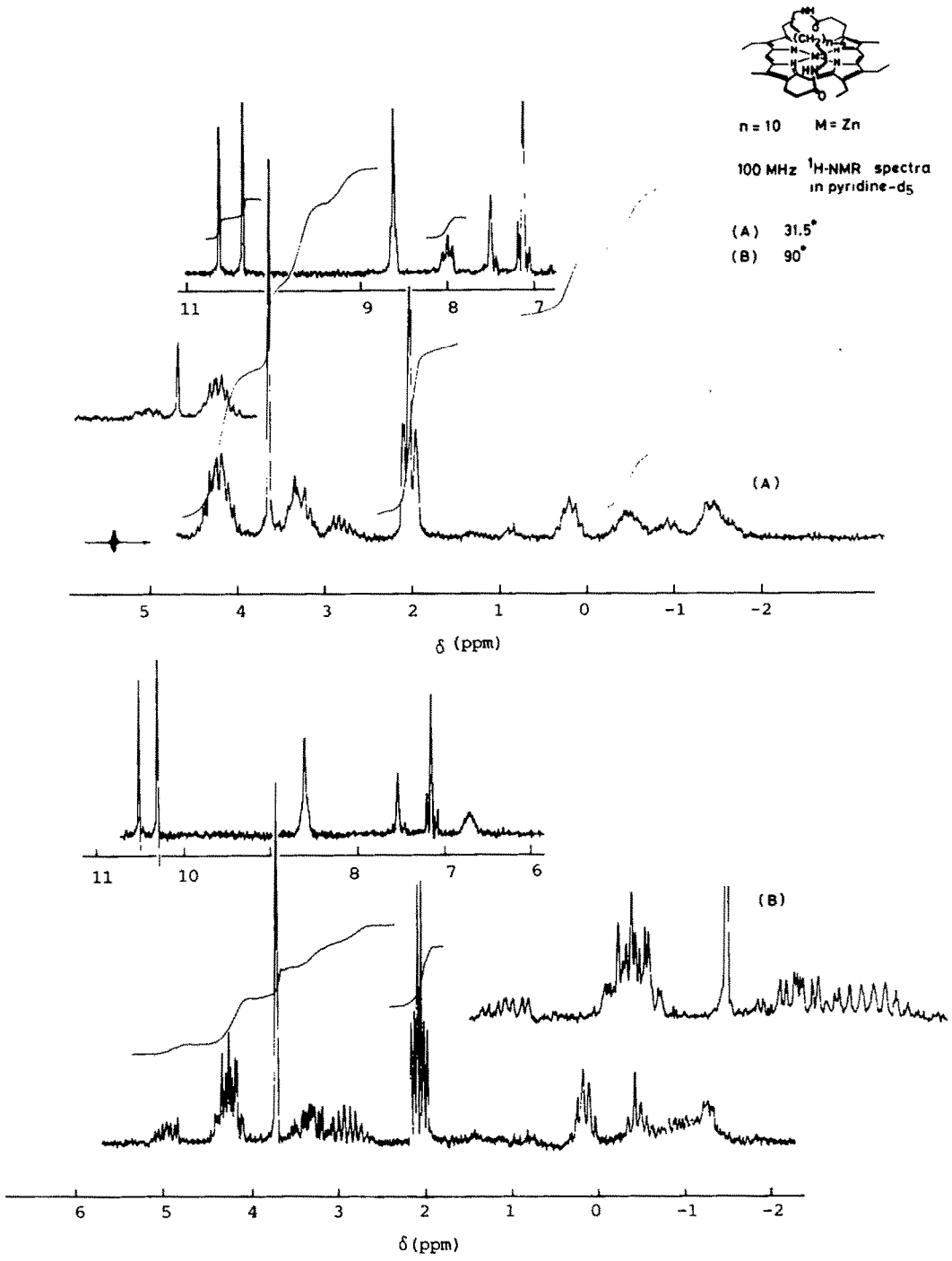

Fig. 3. ^{1}H NMR spectra of [18]-cyclophane porphyrin Zn(II) complex in pyridine-d_5 at 31.5° and 90°.

ambient temperature. Protection from autooxidation of the oxyheme derived from cyclophane heme is not as effective as has been reported for that of the picket-fence heme. The large and rigid amide groups of the picket-fence heme seem to prevent migration of O_2 to the open face to lead to the μ-oxo ferric complex. Non-bonding repulsive interaction between O_2 and the bridged methylene groups may also decrease stability of the oxyheme. Consequently oxygenation (Scheme, 2 F) takes place at the open face of the heme plane to form the μ-oxo ferric complex.

Asymmetric axial ligation

Paramagnetic ^{1}H-NMR spectra of the Fe(III)porphyrins provide important information on their spin states in the solution.[15a] The porphyrinatoFe(III) perchlorate in CH_2Cl_2 was determined to be intermediate spin state by NMR and resonance Raman spectra.[15b, 15c] The spin state of the perchlorate complex varies with polarity of solvent and axial ligation by solvent molecules such as DMSO, MeOH and THF. Weak axial ligands like perchlorate anion are readily replaced by solvent molecules. Table 4 shows paramagnetic ^{1}H NMR

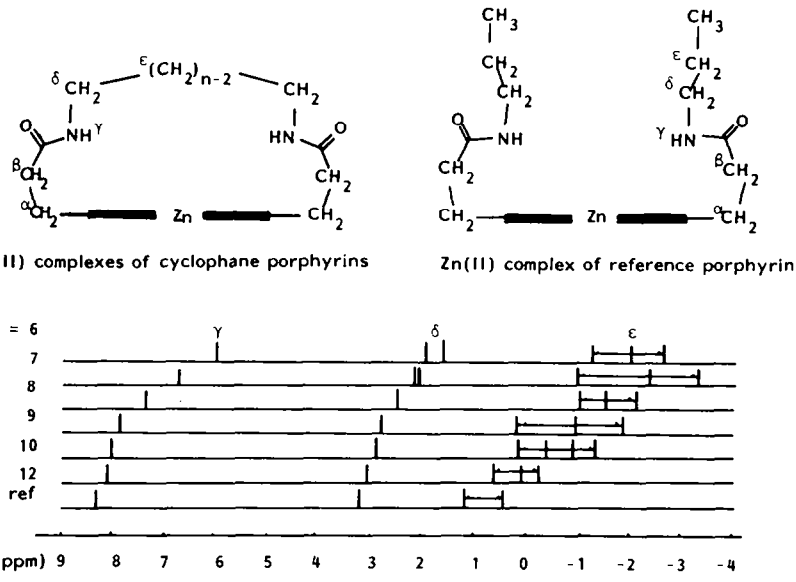

Fig. 4. Positions of chemical shifts of the bridged chain in the cyclophane porphyrin zinc(II) complexes.

spectra of the ferric cyclophane porphyrin complexes in various solvents. It is noted that the perchlorate complexes of non-bridged prophyrins are soluble in aprotic solvents, whereas those of the cyclophane porphyrins are insoluble in aprotic solvents and soluble in protic solvents such as alcohols. As has been mentioned in the crystallographic study of the perchlorate salts, the Fe(III) porphyrin is stacked with an aromatic compound or another Fe(III) porphyrin. A polymethylene group at the bridged face appears to disturb stacking with π-bases or aggregation of metalloporphyrins.

Absorption spectra and ^{1}H NMR spectra of the chloro complexes of ferric [14]-cyclophane porphyrin and the reference porphyrin in $CHCl_3$ demonstrate normal pentacoordination and high spin state. Addition of methanol to the chloroform solution yields asymmetric ligated complexes relative to the 5- and 6th coordination sites. The chloro anion and methanol are axially bound to the ferric complex. Paramagnetic ^{1}H NMR signals of the peripheral CH_3 and α-CH_2 groups of the chloro complex (**25**) in $CDCl_3$ or in $CDCl_3/CD_3OD$ are due to the high spin complex. Those signals of the perchlorate salt (**26**) in $CDCl_3/CD_3OD$ and $CDCl_3$/4Bz-py are different from those of the chloro complex (**26**) in $CDCl_3/CD_3OD$. Absorption spectra of **26** in these mixed solvent systems reveal formation of the high-spin complex. In the $CHCl_3$/MeOH system, replacement of ClO_4^- with CH_3OH and coordination of ClO_4^- from the bridged face generates the hexa-coordinated high-spin complex as shown in Scheme 3 (J). The ESR spectrum of **26** in $MeOH/CH_3Cl_2$ at 77K shows g-values at 5.8 and 2.1 due to the high-spin state.

Table 1. Microanalyses, mass spectra and absorption spectra of the zinc(II) complexes [*m*]-cyclophane porphyrins

Compounds	[m]	Calcd. C(%)	H(%)	N(%)	Found C(%)	H(%)	N(%)	Formula	m/e(M^+)[a]	
(10)	22	70.01	8.05	9.88	70.30	8.05	9.77	$C_{50}H_{68}N_6O_2Zn$	848	402(5.24), 535(4.15) 572(4.23)
(11)[b]	20	76.15	8.52	11.10	75.95	8.58	10.96	$C_{48}H_{66}N_6O_2$	750	401(5.24), 500(4.20), 535(4.04) 568(3.89), 622(3.72)
(12)	18	68.76	7.65	10.46	68.87	7.55	10.60	$C_{46}H_{60}N_6O_2Zn\cdot 1/2(H_2O)$	792	401(5.24), 535(4.15) 573(4.23)
(13)	17	67.70	7.32	10.53	67.71	7.49	9.97	$C_{45}H_{58}N_6O_2Zn\cdot H_2O$	778	402(5.23), 536(4.15) 572(4.23)
(14)	16	67.10	7.38	10.43	67.25	7.61	10.23	$C_{44}H_{56}N_6O_2Zn\cdot 3/2(H_2O)$	764	403(5.22), 537(4.15) 573(4.24)
(15)	15	68.64	7.32	11.17	68.76	7.04	12.07	$C_{43}H_{54}N_6O_2Zn$	750	403(5.22), 535(4.17) 572(4.23)
(16)	14	68.32	7.10	11.38	68.04	7.20	11.11	$C_{42}H_{52}N_6O_2Zn$	736	406(5.24), 537(4.15) 573(4.22)

(a); M^+ indicates parent ion of the zinc complex without solvated water.

(b); [20]-Cyclophane porphyrin was determined as free base.

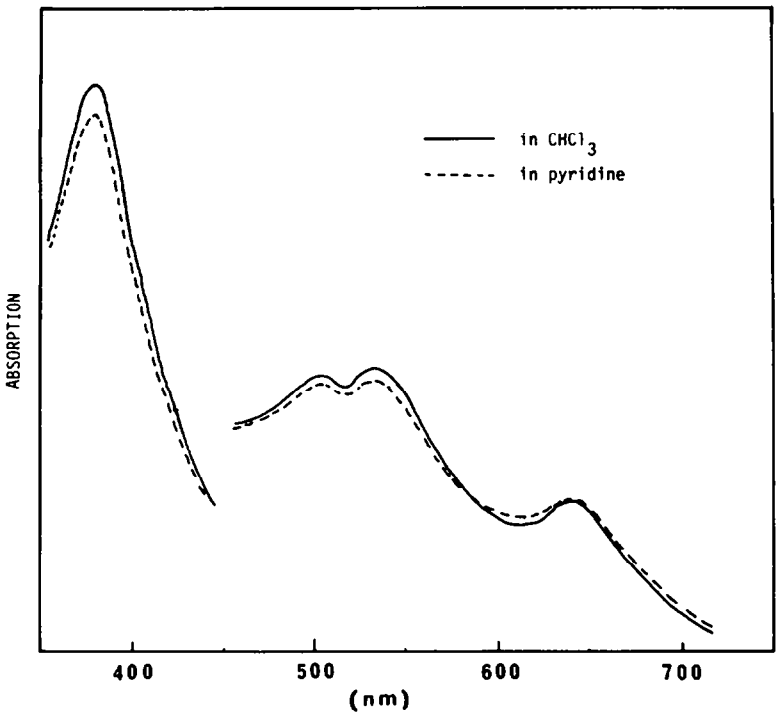

Fig. 5. Absorption spectra of [14]-CP·Fe(III)Cl in $CHCl_3$ (———) and pyridine (----).

However, the ESR measurement in CH_2Cl_2/4-Bz-py did not show clear g-values. This result implies that quantum mechanical admixture of s = 5/2 and 3/2 or intermediate spin state(3/2) cannot be excluded for the cationic complex. Bulky amine molecule is not allowed to coordinate from the bridged face as a sixth ligand. Crystallographic studies of bis-dimethylsulfoxide and bisaquo ferric porphyrins have shown a new type of ferric high spin and hexa-coordinated complex with symmetric axial ligands.[16]

In CH_2Cl_2/4-Bz-py, the first 4-Bz-py molecule is able to ligate from the open face in the place of ClO_4^- (Scheme 3, K). ^1H NMR spectra of the Me group of the complex (**26**) in $CD_3OD/CDCl_3$ and 4-Bz-py/$CDCl_3$ exhibit down-field shifts compared with those of the neutral penta-coordinate high-spin complexes. The perchlorate complex of (**26**) in $CD_3OD/CDCl_3$ shows a linear Curie plot of isotropic shift vs temperature. This fact excludes thermal mixture of low- and high-spin states in the range from $-20°$ to 20°. Addition of 4-Bz-py to the $CHCl_3$ solution of [22]-cyclophane porphyrin Fe(III) complex yields a low-spin and hexa-coordinate complex due to formation of the bisamine complex. Present results suggest that the bridged face is able to recognize the size of axial ligand. Therefore, the complex (**26**) may constitute an asymmetric hexa-coordinate complex formulated as P·Fe(III) (L) (L′) (Scheme 3,

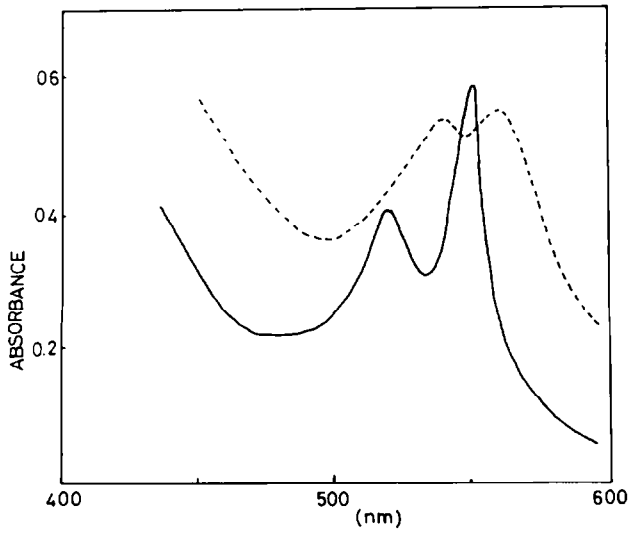

Fig. 6. Absorption spectra of [22]-CP·Fe(II) in benzene-pyridine (2:1 vol/vol)(----) and [14]-CP·Fe(II) in benzene-t-Bu-pyridine (2:1 vol/vol)(———). Concentration of the complexes is 2.5×10^{-5} M.

Table 2. ^{1}H NMR chemical shifts of [*m*]-cyclophane porphyrinatozinc(II)

Assignment	(17)	(10) [m=22]	(11) [m=20]	(12) [m=18]
meso protons	10.50(two singlet, 10.34 4H+4H)	10.54(two singlet, 10.34 4H+4H)	10.57(two singlets, 10.40 4H+4H)	10.61(two singlets, 10.34 4H+4H)
7,17-$CH_2CH_2CONHCH_2$-	8.28(triplet, 2H)	8.08(triplet, 2H)	8.20(triplet, 2H)	8.00(triplet, 2H)
7,17-CH_2CH_2CONH-	4.70(triplet, 4H)	5.00(AA'BB', 4H) 4.60	5.00((AA'BB', 4H) 4.50	5.00((AA'BB', 4H) 4.50
2,3,12,13-CH_2CH_3	4.20(quartet, 8H)	4.16(quartet, 8H)	4.16(quartet, 8H)	4.20(quartet, 8H)
8,18-CH_3	3.69(singlet, 6H)	3.77(singlet, 6H)	3.75(singlet, 6H)	3.64(singlet, 6H)
7,17-CH_2CH_2CONH-	3.39(triplet, 4H)	3.4 (multiplet, 4H)	3.4-3.2 (multiplet, 8H)	3.3-3.5(multiplet, 4H
7,17-$CH_2CH_2CONHCH_2$-	3.20(quartet, 4H)	3.1 (multiplet, 4H)		2.90(multiplet, 4H)
2,3,12,13-CH_2CH_3	1.91(double triplets, 12H)	1.98(double triplet 12H)	1.99(double triplets, 12H)	2.02(double triplets, 12H)
7,17-$CH_2CH_2CONHCH_2CH_2CH_3$	1.20(sextet, 4H) 0.42(triplet, 6H)			
7,17-$CH_2CH_2CONHCH_2(CH_2)_{m-10}$-		0.9-0.3(broad multiplet, 24H)	0.70 0.10(three broad -0.4 multiplets, 20H)	0.2 -0.5(four broad -1.0 multiplets, -1.4 16H)

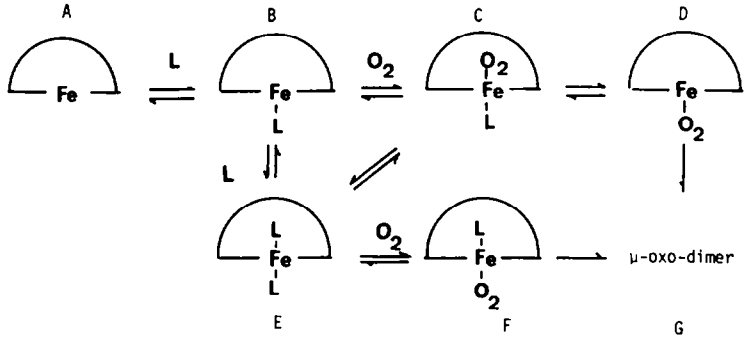

Scheme 2.

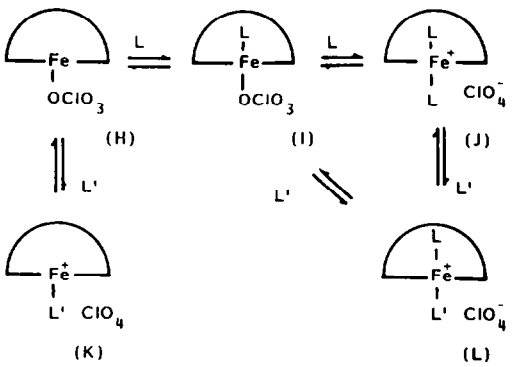

L= CH_3OH

L' = 4-Benzylpyridine

Scheme 3.

L). Weak axial ligand such as ClO_4^- can be readily replaced with strong ligands or protic solvent molecule. The high solubility of **26** in MeOH suggests formation of H-bonds between the coordinated MeOH and ClO_4^-. In the case of the chloro hemin, Cl^- tightly bonded to the hemin is dissociable and exchangable with strong ligands. As is shown in ^{1}H NMR spectrum, it is unlikely that the Cl^- is completely substituted with MeOH. In two mixed solvent systems, it seems that the strong ligand 4-Bz-py coordinates to the ferric complex (**26**) from the open-face due to steric constraint and the weak ligand MeOH ligates the bridged face without steric repulsion. The signals of the Me group in the present system differ from those of the symmetric hexa-coordinate and penta-coordinate high spin complexes. Prosthetic protoheme in the oxidized hemoproteins is usually coordinated with the imidazole of

and reference porphyrinatozinc(II) in pyridine-d_5

(13) [m=17]	(14) [m=16]	(15) [m=15]	(16) [m=14]
10.47(two singlets, 10.33 4H+4H)	10.37(two singlets, 10.25 4H+4H)	10.57(two singlets, 10.39 4H+4H)	10.41(two singlets, 10.36 4H+4H)
7.81(triplet, 2H)	7.27(triplet, 2H)	6.64(triplet, 2H)	5.94(triplet, 2H)
4.90(AA'BB', 4H) 4.50	4.80(AA'BB', 4H) 4.50	5.04(AA'BB', 4H) 4.20	4.82(AA'BB', 4H) 4.40
4.16(double quartets 4H+4H)	4.12(double quartets, 4H+4H)	4.20(double quartets, 4H+4H)	4.18(double quartets, 4H+4H)
3.64(singlet, 6H)	3.57(singlet, 6H)	3.52(singlet, 6H)	3.64(singlet, 6H)
3.24(multiplet, 4H)			3.1-2.8(multiplet, 4H)
2.90(multiplet, 4H)	3.2-2.8 (multiplet, 8H)	3.0-2.3 (two multiplets, 8H)	2.0-1.6(multiplet, 4H)
2.00(double triplets 12H)	1.95(double triplets 12H)	2.10(double triplets, 12H)	1.94(double triplets, 12H)
0.2 -1.0(three broad -1.4 multiplets, 14H)	-1.2--2.6 (four broad multiplets, 12H)	-1.0 -2.5 (three broad -3.4 multiplets, 10H)	-1.4 -2.1 (three broad -2.7 multiplets, 8H)

the proximal histidine and probably with H_2O. Consequently the present intermediate presented by (L) in Scheme 3 seems to be an analogue of metmyoglobin and methemoglobin.

(B) Cobalt(II) complexes of the bridged porphyrins

Co(II) complexes are particularly interesting as analogues of the heme and hemoproteins.[17] The Co(II) complexes of the bridged porphyrins reversibly bind O_2 at room temperature. Fig. 7 shows the absorption spectra of the Co(II) complex of the bridged porphyrin during oxygenation. The absorption spectrum under anaerobic condition shows bands at 339 and 550 nm due to the deoxy form.[17] Introduction of 1 atm O_2 to a DMF solution of the [20]-cyclophane porphyrin complex generates new absorptions at 425, 540 and 565 nm. Their absorption intensities increases with the six isosbestic points. It is noted that the rate of oxygenation of the Co(II) complexes is dependent on the size of the bridged chain. Monitoring of oxygenation by absorption spectra indicates that the initial rate increases with the size of the bridged chain. The slower rate of oxygen binding to porphyrin complexes with shorter bridges is ascribed to repulsive interactions between the bridged group and O_2. The reference Co(II) complex is expected to bind O_2 more rapidly than the bridged porphyrin complexes. The complexes with larger chains show, however, higher rates than the reference complex. This fact suggests that the rate enhancement of oxygenation is due to desolvation of the solvent molecules from near proximity of the Co(II) ion.[18] Collman *et al.* have reported marked effect of solvation on the oxygenation of the Co(II) complexes.[19] Table 5 summarizes the ESR parameters of the Co(II) bridged porphyrins in dimethylformamide at 77 K. Comparison of the parameters of the bridged complexes with those of the reference complex shows no significant differences among them. These values provide evidence of formation of five coordinated and square pyramidal Co(II) complexes of the low spin state.[19] Oxygenation of the Co(II) complexes gives new signals characteristic of the free radical type with axial symmetry ($g = 2.00$ and 2.09). These parameters are also consistent with those of oxygenated complexes previously reported.[20]

CONCLUSION

Axial ligation of the residue of amino acids to the prosthetic heme in the hemoproteins and heme enzymes is very important to control their redox potentials and catalytic functions. They have usually two different axial ligands involving external ligands except for cytochrome b_5. Furthermore, in some heme enzymes axial ligand does not coordinate to the heme along the vertical line through the Fe atom. Unlike usual iron porphyrins, cyclophane porphyrins enable us to construct the Fe complexes asymmetrically coordinated with different ligands. Metal complexes of the cyclophane porphyrins having various size of bridged chains differentiates the size of axial ligands at the bridged face and causes hindered axial ligation. Present model systems provide more elaborate model to mimic the structure in proximity of the prosthetic heme for the heme enzymes and hemoproteins.

Table 3. Yields, elemental analysis, IR and UV absorption spectra of [*m*]-cyclophane porphyrinatoiron(III)chlorides and [*m*]-cyclophane porphyrinatocobalt(II)

[m]Cyclophane porphyrinatoiron(III)chlorides:

[m]	Compound	Yield(%)	Formula	Elemental analysis Calcd(Found)	Infrared spectra(cm^{-1})	Absorption spectra λmax(nm) (logε)
22	(19)	90	$C_{50}H_{68}N_6O_2FeCl$	C, 68.52(68.61) H, 7.82(8.00) N, 9.58(9.33)	3300 1640 1550(amide)	380(4.76) 508(3.80) 537(3.82) 638(3.50)
20	(20)	97	$C_{48}H_{64}N_6O_2FeCl$	C, 67.95(67.89) H, 7.60(7.85) N, 9.90(9.14)	3300 1645 1550(amide)	380(4.77) 509(3.81) 536(3.81) 638(3.50)
18	(21)	95	$C_{46}H_{60}N_6O_2FeCl\cdot(H_2O)3/2$	C, 65.20(65.16) H, 7.49(7.12) N, 9.91(9.14)	3310 1645 1555(amide)	380(4.76) 508(3.79) 537(3.81) 639(3.51)
17	(22)	85	$C_{45}H_{58}N_6O_2FeCl$	C, 67.03(66.94) H, 7.25(7.19) N, 10.42(9.92)	3300 1640(broad) 1550(amide)	381(4.70) 509(3.80) 537(3.80) 639(3.84)
16	(23)	82	$C_{44}H_{56}N_6O_2FeCl$ (H_2O)	C,65.22(65.21) H, 6.97(7.07) N,10.37(10.36)	3300 1640(br) 1550(br,amide)	380(4.89), [illegible] 508(3.81) 537(3.82) 638(3.51) 400(4.78) 506(3.65) 536(3.64) 636(3.31) (py)
15	(24)	85	$C_{43}H_{54}N_6O_2FeCl$ $(H_2O)1/2$	C,65.60(65.48) H, 7.03(6.90) N,10.66(10.64)	3300 1640(br) 1550(br,amide)	380(4.88) 507(3.79) 538(3.81) 639(3.49)
14	(25)	89	$C_{42}H_{52}N_6O_2FeCl$ $(H_2O)3/2$	C,63.75(63.67) H, 7.00(6.81) N,10.62(10.14)	3300(br) 1640(br) 1550(br,amide)	380(4.77) 506(3.87) 535(3.88) 638(3.51) 381(4.77) 505(3.87) 535(3.88) 638(3,51) (py)
14	(26)	65	$C_{42}H_{52}N_6O_6FeCl\cdot1/2CH_3OH$	C, 63.75(63.67) H, 7.00 (6.81) N, 10.62(10.14)	1140, 1105 1080(ClO_4^-)	390(4.83)[b] 500(4.01) 613(3.61)
17	(27)	73	$C_{45}H_{58}N_6O_6FeCl$	C, 62.10(61.85) H, 6.72 (6.70) N, 9.66 (9.54)	1140, 1105 1080(ClO_4^-)	394(4.85)[b] 494(4.00) 615(3.62)
ref.[a]	(28)	80	$C_{40}H_{48}N_4O_8$	C, 59.80(59.61)	1725(ester)	387(4.83)

Table 3. (*Contd*)

[m]	Compound	Yield(%)	Formula	Elemental analysis CalCalcd(Found)	Infrared spectra(cm^{-1})	Absorption spectra λ max(nm) (log ϵ)
				H, 6.02 (5.99) N, 6.97 (6.76)		495(4.02)
[m]Cyclophane porphyrinatocobalt(II):						
22	(30)	81	$C_{50}H_{68}N_6O_2Co$	C, 71.15(71.04) H, 8.12(8.19) N, 9.95(9.84)	3300 1640 1550(amide)	394(5.38) 518(4.02) 555(4.44)
20	(31)	83	$C_{48}H_{64}N_6O_2Co$	C, 70.65(70.38) H, 7.90(8.17) N, 10.29(10.30)	3300 1645 1550(amide)	394(5.39) 518(4.11) 555(4.48)
18	(32)	85	$C_{46}H_{60}N_6O_2Co$	C, 70.11(70.34) H, 7.67(7.60) N, 11.26(10.45)	3300 1645 1650(amide)	394(5.37) 518(4.12) 555(4.43)
15	(33)	80	$C_{43}H_{54}N_6O_2Co$	C, 69.24(69.08) H, 7.29(7.60) N, 11.26(10.45)	3300(br) 1640(br) 1550(br,amide)	393(5.31) 518(4.13) 555(4.43)

a) ref. shows ferric perchlorate complex of (6)

b) Absorption spectra were measured in CH_2Cl_2-CH_3OH (v/v, 10/1)

EXPERIMENTAL

Synthesis of materials

3'-(2-Carboxyethyl)-3,4-diethyl-4',5'-dimethyl-2,2'-dipyrryl methene hydrobromide (**3**). A ethanolic soln 3 ml of **1** (1.00 g) and **2** (0.67 g) containing 48% HBr (1.3 ml) was allowed to stand for 30 min at −10°. The crystalline product was collected by filtration, washed with ether and dried under vacuum. Recrystallization from EtOH–petroleum ether gave orange red crystals (2.0 g) in 66% yield, m.p. 128°; IR 1718 cm^{-1} (ν_{CO} for ester group); PMR $\delta(CDCl_3)$ 1.21(m, 6H, 3,4-CH_2CH_3), 2.05(s, 3H, 4'-CH_3), 2.63(m, 3H, 3'-CH_2CH_3), 7.58(d, 1H, 5- =CH–), 7.99(br s, 1H methine proton), 13.05(br s, 2H, NH); vis($CHCl_3$) λ_{max}(log ϵ_{max}) 371(3.21), 456(4.49), 482(4.83). (Found: C, 57.08, H, 6.33; N, 7.94; O, 7.80; Br, 20.84. Calc. for $C_{18}H_{25}N_2O_2Br$: C, 56.69; H, 6.60; O, 7.43; Br, 20.95%).

Table 4. Paramagnetic proton chemical shifts of ferric complexes[a]

Complex		Solvent	8.18-CH_3	7,17-CH_2CH_2	2,3,12,13-CH_2CH_3
[14]-CP·Fe(III)Cl	(25)	$CDCl_3$-CD_3OH	46.5	42.9	37.5
rP·Fe(III)Cl	(29)	$CDCl_3$	48.7	42.6	39.4
[22]-CP-Fe(III)·-ClO_4	(26)	$CDCl_3$-CD_3OD	61.4	46.5	43.3 42.3
		$CDCl_3$ -4-benzyl-py	61.2	45.3	40.3
rP-Fe(III)-ClO_4	(28)	$CDCl_3$	55.0	31.8	

[m]-CP and rP denote the [m]-cyclophane porphyrin and reference porphyrin

a) Chemical shifts are shown with respect to internal TMS.

Table 5. EPR parameters of deoxy and dioxygen complexes of the cobalt(II) porphyrins[a]

Complex	$g_{\perp}$	$g_{\parallel}$	$A_{\parallel}$(Co)	$A_{\parallel}$(N)
[22]-CP-Co(II)·(N-ethylimidazole)	2.34	2.03	81.3	17.5
" + O_2	2.00	2.09	18.0	
[18]-CP-Co(II)·(N-ethylimidazole)	2.34	2.03	81.4	16.3
" + O_2	2.00	2.09	18.4	
[15]-CP-Co(II)·(N-ethylimidazole)	2.34	2.03	81.1	16.3
" + O_2	2.00	2.09	18.4	
rP·Co(II)·(N-ethylimidazole)	2.37	2.06	74.3	17.0
" + O_2	2.00	2.08	20.0	

a) Spectra were measured in dimethylformamide/N-methylimidazole at 77 K. CP and rP denote the cyclophane and referenceporphyrins respectively.

5-Bromo-5'bromomethyl-3,4-diethyl-3'-(2-carboxyethyl)-4'-methyl-2,2'dipyrrylmethene hydrobromide **4**. A suspension of **3** (0.95 g) in glacial AcOH (16 ml) containing Br_2 (0.42 ml) was heated at 80–90° for 1 hr. After cooling, fine crystals were collected. Recrystallization from glacial AcOH gave red needles (0.67 g) in 50% yield, dec. at 134°; IR 1738 cm^{-1} ($\nu_{C=O}$); PMR $\delta(CD_3OD)$ 0.85(t, 3H, 3-CH_2CH_3), 1.21 (t, 3H, 4-CH_2CH_3), 1.69 (s, 3H, 4-CH_3), 2.40 (m, 8H, 3,4-CH_2CH_3 and 3'-$CH_2CH_2CO_2$–), 4.43 (s, 2H, 5'–CH_2Br), 7.39 (s, 1H, methine proton); vis (CH_2Cl_2) λ_{max} (log ϵ_{max}) 374 (3.83), 505 (4.89). (Found: C, 40.09; H, 4.47; N, 4.87; O, 5.58; Br, 44.12. Calc. for $C_{18}H_{23}N_2O_2Br_3$: C, 40.10; H, 4.30; N, 5.19; O, 5.93; Br, 44.46%).

1-Bromo-1, 19-dideoxy-7, 17-di (2-ethoxycarbonylethyl)-2,3,12,13-tetraethyl-8,18,19-trimethyl-biladiene-a,c-dihydrobromide (**5**). A mixture of **3** (500 mg) and **4** (710 mg) in dry CH_2Cl_2 (20 ml) was treated with anhyd $SnCl_4$ (1.2 ml) in one portion and kept for 20 hr at room temp. The solvent was removed under reduced pressure. The residue was treated with a mixture of EtOH (50 ml) and conc HBr (20 ml). After heating at 45° for 30 min, the soln was poured into water and extracted with $CHCl_3$. The extract was dried over $MgSO_4$ and solvent was removed under reduced pressure. Crystallization of the residue from $CHCl_3$-ether gave red brown prisms (1.08 g) in 90% yield: dec. at 182°; IR 1730 cm^{-1}; PMR $\delta(CDCl_3)$ 1.20 (m, 18H, 2,3,12,13-CH_2CH_3 and 7,17-$CO_2CH_2CH_3$), 1.87 (s, 3H, 8-CH_3), 2.01 (s, 3H, 18-CH_3), 2.65 (m, 19H, 19-CH_3, 2,3,12,13-CH_2CH_3 and 7,17-$CO_2CH_2CH_3$), 4.0 (m, 4H, 7,17-$CH_2CH_2CO_2$), 5.18 (s, 2H, 10-CH_2–), 7.33 (s, 2H, 5,15-CH=), 13.5 (br s, 4H, NH); vis (CH_2Ci_2) λ_{max}(log ϵ_{max}) 376 (4.15), 462 (5.42), 555 (5.17), 496 (4.49). (Found: C, 53.54; H, 6.31; N, 6.33; O, 7.35; Br, 27.31. Calc. for $C_{41}H_{55}N_4O_4Br_3$: C, 54.25; H, 6.10; N, 6.17; O, 7.05; Br, 26.41%).

Diethyl 7,8,17,18-*tetraethyl*-3,13-*dimethylporphyrin*-2,12-

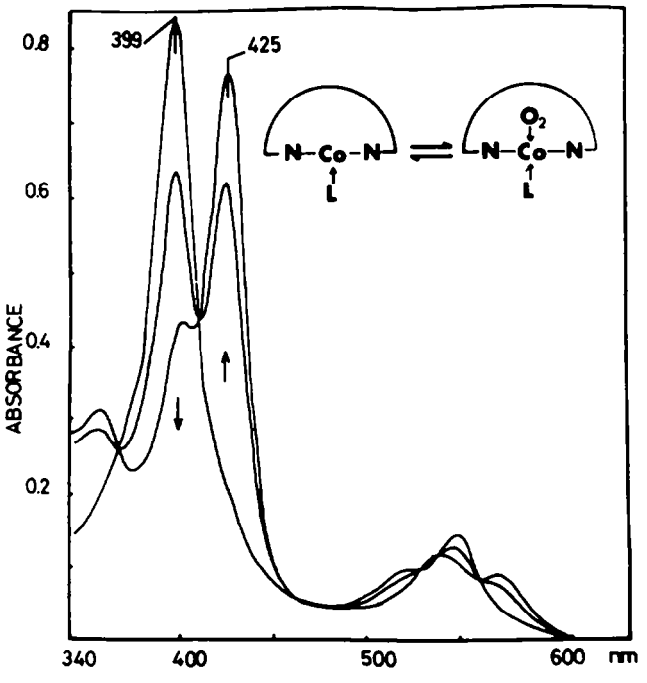

Fig. 7. Absorption spectra of [20]-CP·Co(II) (10 mg) in DMF-N-ethylimidazole (10 ml, 9:1 vol/vol).

dipropionate **6**. Salt **5** (75 mg) was suspended in *o*-chlorobenzene (26 ml) and heated under reflux with aeration for 20 min. The solvent was evaporated under reduced pressure, and the residue was chromatographed on an alumina column with $CHCl_3$ as eluent. The fraction containing the porphyrin was evaporated under vacuum. Recrystallization from $CHCl_3$-MeOH gave purple red crystals (30 mg) in 56% yield, m.p. 212°; IR 1725 cm^{-1} (ν_{CO}); PMR $\delta(CDCl_3)$ −4.4 (br s, 2H, NH), 1.10 (t, 6H, 2,12-$CO_2CH_2CH_3$), 2.19 (m, 12H, 7,8,17,18-CH_2CH_3), 3.47 (t, 4H, 2,12-$CH_2CH_2CO_2$), 4.55 (s, 6H, 3,13-CH_3), 4.00 (m, 12H, 7, 8, 17, 18-CH_2CH_3 and 2,12-$CH_2CH_2CO_2$), 4.25 (t, 4H, 2,12-$CH_2CH_2CO_2$), 10.03 (s, 4H, meso proton); vis ($CHCl_3$) λ_{max} (log ϵ_{max}) 400 (5.15), 499 (3.98), 567 (3.68) and 620 nm (3.55). Found: C, 73.39; H, 7.68; N, 8.48; O, 10.13. Calc. for $C_{40}H_{30}N_4$: C, 73.81; H, 7.74; N, 8.61; O, 9.83%).

7,8,17,18-*Tetraethyl*-3,13-*dimethylporphyrin*-2,12-*dipropionic acid* (**7**). Ester **6** (100 mg) was suspended for 20 hr in 5% HCl and extracted with $CHCl_3$. The $CHCl_3$ extract was washed with water and dried over Na_2SO_4. The $CHCl_3$ was removed under reduced pressure and the residue was crystallized from pyridine-MeOH to give fine purple red crystals (89.5 mg) in 98% yield, IR 1700 cm^{-1} (ν_{CO}); PMR δ (pyridine-d_5) 2.00 (m, 12H, 7,8,17,18-CH_2CH_3), 3.80 (s, 6H, 3,13-CH_3), 4.00 (m, 12H, 7,8,17,18-CH_2CH_3 and 2,12-$CH_2CH_2CO_2$), 4.50 (t, 4H, 2,12-$CH_2CH_2CO_2$), 10.50 (s, 2H, meso protons) 10.70 (s, 2H, meso protons); vis-(pyridine) λ_{max}(log ϵ_{max}) 401 (5.22), 497 (4.15), 530 (3.99), 566 (3.83) and 620 nm (3.66). (Found: C, 73.01; H, 6.81; N, 11.25. Calc. for $C_{36}H_{42}N_4O_4 \cdot C_6H_5N$: C, 73.08; H, 7.03; N, 10.39%).

7,8,17,18-*Tetraethyl*-3,13-*dimethylporphyrin*-2,12-*dipropanol* (**8**). To a tetrahydrofuran soln (100 ml) of **6** (100 mg) was added $LiAlH_4$ (100 mg) in one portion under N_2 and stirred for 1 hr. The mixture was poured into water and extracted with CH_2Cl_2. The extract was washed with water and dried over $MgSO_4$. The solvent was removed under reduced pressure. The residual solid was crystallized from $CHCl_3$-MeOH to give hygroscopic purple red crystals (82 mg) in 95% yield, PMR δ (pyridine-d_5) 1.90 (t, 12H, 7,8,17,18-CH_2CH_3), 1.50 (quintet, 4H, 2,12-$CH_2CH_2CH_2Br$), 3.66 (singlet, 6H, 3,13-CH_3), 4.30 (multiplet, 16H, 2,3,12,13-CH_2CH_3 and 2,12-$CH_2CH_2CH_2CH_2Br$), 10.55 (s, 2H, meso), 10.50 (s, 2H, meso protons), vis (pyridine λ_{max} (log ϵ_{max}) 403 (4.89), 499 (4.13), 533 (3.97), 569 (3.79) and 625 nm (3.45). (Found: C, 62.81; H, 6.43; N, 7.83. Calc. for $C_{36}H_{38}N_4Br_2$: C, 62.43; H, 6.40; N, 8.09%).

Cyclophane porphyrins **10–16**

General procedure. To a tetrahydrofuran soln (20 ml) of **7** (100 mg) with 0.05 ml Et_3N was added isobutylchloroformate (0.06 ml) at 0° and stirred for 1 hr at room temp. To this prepared mixed anhydride soln was added very slowly a tetrahydrofuran soln of the diamine [100 mg, $H_2N(CH_2)_nNH_2$, n = 6,7,8,9,10,12,14] and stirred for 20 hr. The solvent was evaporated under reduced pressure. The residue was dissolved in pyridine-MeOH (20 ml of 1:1 vol/vol) containing zinc acetate (50 mg) was warmed at 50° until the color of the soln was turned from purple red to orange red. The solvent was removed under reduced pressure. The residual solid was chromatographed by preparative TLC (Merck Co. silica gel. 60 F_{254}) with acetone-CH_2Cl_2 (1:3 vol/vol) as eluent. The bridged porphyrinato Zn(II) complexes appeared at about R_f = 0.6–0.7. The orange red zone was collected and extracted with acetone–CH_2Cl_2. The extract was condensed to small portion and crystallization of the residual solid from pyridine-MeOH afforded purple red crystals (30–60 mg). Yields, elemental analyses, mass spectra and absorption spectra of the cyclophane porphyrinato Zn(II) complexes are summarized in Table 1.

The reference porphyrins were prepared according to the same general procedure, using primary amines [$CH_3(CH_2)_nNH_2$, n = 2 and 5] instead of daimines:

N,N'-Dipropyl-7,8,17,18-*tetraethyl*-3,13-*dimethylporphyrin*-2,12-*dipropionamide zinc(II) complex* (**17**) in 89% yield; IR 3300, 1645 and 1555 cm^{-1} (amide); vis($CHCl_3$) λ_{max}(log ϵ_{max}) 401 (5.24), 535 (4,14), and 572 nm (4.23). (Found: C, 68.09; H, 7.34; N, 11.54. Calc. for $C_{42}H_{54}N_6O_2Zn$: C, 68.14; H, 7.35; N, 11.35%).

N,N'-Dihexyl-7,8,17,17-*tetraethyl*-3,13-*dimethylporphyrin*-2,12-*di-propionamide* (**18**) in 92% yield; IR 3300, 1645 and 1555 cm^{-1} (amide); vis ($CHCl_3$) λ_{max} (log ϵ_{max}) 401 (5.24), 500 (4.20), 535 (4.08), 568 (3.89), and 622 nm (3.73). (Found: C, 76.02; H, 8.58; N, 10.98. Calc. for $C_{48}H_{68}N_6O_2$: C, 76.14; H, 8.54; N, 11.09%).

PMR data for these reference porphyrins are summarized in Table 2.

Chloro complexes of the ferric cyclophane porphyrins **19–25**

General procedure. [*m*]-Cyclophane porphyrinato Zn(II) (50 mg) were dissolved in glacial AcOH (10 ml). To the soln was added ferrous acetate (50 mg, prepared from 1g of reduced Fe powder in 50 ml of glacial AcOH). The mixture was heated at 70° for 30 min. The soln was poured into water containing 2 g NaCl and extracted with benzene. The benzene extract was washed with water and dried over Na_2SO_4. The solvent was removed under reduced pressure. Crystallization of the residue from benzene gave brown red crystals in quantitative yields. Their yields, IR, visible spectral data and micro analyses are summarized in Table 3.

Syntheses of the perchlorates (**26–28**). The chloro Fe(III) porphyrin (30 mg) was dissolved in 20 ml of freshly distilled CH_2Cl_2. To the soln was added 30 mg of $AgClO_4$ and 10 ml of MeOH. The mixture was refluxed for 30 min under argon and cooled to room temp. The ppt of AgCl was removed by filtration. The filtrate was evaporated under reduced pressure. The residue was dissolved in dry benzene and kept for several days. The resulting crystals were washed with petroleum ether and dried over P_2O_5 at 60°.

Cobalt(II) complexes of the bridged porphyrins

General procedure. The [*m*]-bridged porphyrinato Zn(II) (50 mg) complex was dissolved in a small amount of pyridine. The pyridine soln was diluted with CH_2Cl_2 (50 ml). The soln was poured into 100 ml 5% HCl and extracted with CH_2Cl_2. The extract was washed with water and dried over Na_2SO_4. The solvent was removed under reduced pressure. The residue was dissolved in DMF (20 ml) containing cobaltous acetate (20 mg) and heated at 60-70° for 1 hr under argon. After removal of solvent under reduced pressure, the residue was chromatographed on a silica gel column eluted with CH_2Cl_2 acetone (6:1 vol/vol). The first red zone was collected and the solvent was removed under reduced pressure. Crystallization of the residual solid afforded purple red crystals. Micro-analyses and spectral properties are listed in Table 3. Fe(III) and Co(II) complexes of the reference porphyrins were synthesized according to the general procedures for the bridged porphyrin Fe(III) and Co(II) complexes.

N, N'-Dihexyl-7, 8, 17, 18-*tetraethyl*-3, 13-*dimethylporrin*-2,12-*dipropionamide iron*(III) *chloride* (**29**). 59 mg in 97% yield; IR 3300, 1645, and 1550^{-1} (amide); vis($CHCl_3$) λ_{max} (log ϵ_{max}) 381 (4.76), 505 (3.87), and 638 nm(3.52). (Found: C, 68.50; H, 8.03; N, 9.50. Calc for $C_{48}H_{66}O_2FeCl$: C, 67.80; H, 7.82; N, 9.88%).

N, N'-Dihexyl-7, 8, 17, 18-*tetraethyl*-3, 13-*dimethylporphyrin*-2,12-*dipropionamide cobalt*(II) (**34**). 45 mg in 91% yield; IR 3300, 1645 and 1550 cm^{-1} (amide). (Found: C, 70.32; H, 7.54; N, 10.50. Calc. for $C_{48}H_{66}N_6O_2Co$: C, 70.48; H, 8.31; N, 10.27%).

Preparation of ferrous complexes of cyclophane porphyrins, [*m*]-Cyclophaneporphyrinato Fe(III) chloride (10 mg) was dissolved in CH_2Cl_2-N-ethylimidazole (10 ml, 9:1 vol/vol). The soln was degassed completely by the freez-thaw method. To the soln was added degassed water (10 ml, phosphate buffer pH = 7) containing a small amount of sodium dithionite and stirred for 1 hr. The resulting orange

red soln was filtered under argon. The aqueous layer was removed from the soln by syringe and the resulting orange soln was used for spectral measurements. Toluene soln of the ferrous complexes were prepared according to the following method; [m]-Cyclophane porphyrinato Fe(III) chloride (10 mg) was dissolved in toluene-N-ethylimidazone (10 ml, 9:1 vol/vol). The soln was degassed by the freeze-thaw method. To the soln was added a small portion of $NaBH_4$ followed by further stirring for 1 hr. The orange soln was filtered under argon. The absorption spectra were recorded on a Varian 635 spectrophotometer with an Oxford variable temp. liquid N_2 cryostat. The ^1H NMR spectra were recorded on a JEOL FX-90 FT-NMR spectrometer operating at 59.5 MHz. Typically 2000 scans were collected using a 20 μs 90° pulse. The ESR spectra were measured on JEOL JES-FE3X spectrometer at 77K. Absorption spectra were obtained by using Hitachi spectrophotometer Model 340.

REFERENCES

[1]A part of this work was presented in Japan-U.S.A. Joint Seminar at Hawaii (1975).

[2a]Department of Material Science, Technological University of Nagaoka, Nagaoka, Ni-igata, 949-54 Japan; [b]Department of Chemistry, Osaka City University, Sugimotocho, Sumiyoshi, Osaka, 558 Japan; [c]Department of Synthetic Chemistry, Sakyo, Kyoto 606 Japan.

[3a]J. P. Collman, R. R. Gagne, C. A. Reed, T. R. Halbert, G. Lang and W. T. Robinson, *J. Am. Chem. Soc.* **97**, 1427 (1975); [b]J. P. Collman, *Acc. Chem. Res.* **10**, 265 (1977); [c]G. B. Jameson, F. S. Molinaro, J. A. Ibers, J. P. Collman, J. I. Brauman, E. Rose and K. S. Suslick, *J. Am. Chem. Soc.* **102**, 3224 (1980).

[4a]J. Almog, J. E. Baldwin, R. L. Dyer, M. Peters, *Ibid.* **97**, 226 (1975); [b]J. R. Budge, P. E. Ellis, Jr., R. D. Jones, J. E. Linard, F. Basolo, J. E. Baldwin, R. L. Dyer, *Ibid.* **101**, 4762 (1979); [c]G. B. Jameson, J. A. Ibers, *Ibid.* **102**, 2823 (1980); [d]T. Hashimoto, R. L. Dyer, M. T. Crossley, J. E. Baldwin and F. Basolo, *Ibid.* **104**, 2101 (1982).

[5]N. E. Kagan, D. Mauzerall and R. B. Merrifield, *Ibid.* **99**, 5484 (1977).

[6]T. G. Traylor, C. K. Chang, J. Geibel, A. Berzinis, T. Mimcey and J. Cannon, *Ibid.* **101**, 6716 (1979).

[7a]H. Ogoshi, H. Sugimoto and Z. Yoshida, *Tetrahedron Lett.* 4477 (1976); [b]H. Ogoshi, H. Sugimoto and Z. Yoshida, *Ibid.* 4481 (1976); [c]H. Ogoshi, H. Sugimoto and Z. Yoshida, *Ibid.* 1515 (1977).

[8]A. R. Battersby, D. G. Buckley, S. G. Hartley and M. D. Turnbull, *J. Chem. Soc.* Chem. Commun. 879 (1976).

[9]C. K. Chang, *J. Am. Chem. Soc.* **99**, 2819 (1976).

[10a]C. K. Chang and M. S. Kuo, *Ibid.* **101**, 3413 (1979); [b]B. Ward, C. Wang and C. K. Chang, *Ibid.* **103**, 5236 (1981).

[11]M. Momenteau, B. Coock, J. Mispelter, E. Bisagni, *Nouveau, J. Chem.* **3**, 77 (1979).

[12]A. Battersby and A. D. Hamilton, *J. Chem. Soc.* Chem. Commum. 117 (1980).

[13]H. Ogoshi, H. Sugimoto, S. Sanada, E. Watanabe and Z. Yoshida, *Chem. Lett.* 427 (1975).

[14]H. Ogoshi, J. Setsune, T. Omura and Z. Yoshida, *J. Am. Chem. Soc.* **97**, 6461 (1975).

[15]G. N. LaMar and F. A. Walker, *The Porphyrins* (Edited by D. Dolphin), Vol. IV, p. 61. Academic Press, New York (1979).

[16a]M. E. Kastner, W. R. Scheidt, T. Mashiko and C. A. Reed, *J. Am. Chem. Soc.* **100**, 666 (1978); [b]T. Mashiko, M. E. Kastner, K. Spartalian, W. R. Scheidt and C. A. Reed, *Ibid.* **100**, 6354 (1978); [c]W. R. Scheidt, I. A. Cohen and M. E. Kastner, *Biochemistry* **18**, 3546 (1979).

[17a]B. M. Hoffman, D. H. Petering, *Proc. Natl Acad. Sci. U.S.A.* 67, 634 (1970); [b]C. A. Spilburg, B. M. Hoffman and D. H. Petering, *J. Biol. Chem.* **247** 4219 (1972).

[18]P. E. Ellis Jr., J. E. Linard, T. Szymanski, R. D. Jones, J. R. Budge and F. Basolo, *J. Am. Chem. Soc.* **102**, 1889 (1980).

[19]J. P. Collman, J. I. Brauman, K. M. Doxsee, T. R. Halbert, S. E. Hayes and K. S. Suslick, *Ibid.* **100**, 2761 (1978).

[20a]F. A. Walker, *Ibid.* **95**, 1154 (1973); [b]R. M. Guidry and R. S. Drago, *Ibid.* **95**, 6645 (1973).